

In Situ Observations of Toughening Processes in Alumina Reinforced with Silicon Carbide Whiskers

Jürgen Rödel,* Edwin R. Fuller, Jr.* and Brian R. Lawn*

Ceramics Division, National Institute of Standards and Technology, Gaithersburg, Maryland 20899

An in situ study is made of crack interfaces in composites of alumina reinforced with silicon carbide whiskers. Both qualitative observations of the whisker-bridging micromechanisms and quantitative measurements of the crack profile are made to assess the specific role of the whiskers on the toughness curve (*T*-curve or *R*-curve). At small crack-wall separations the whiskers act as elastic restraints to the point of rupture. In some cases the whiskers remain in frictional contact with the alumina matrix over large pullout distances (more than 1 μm) corresponding to a bridging zone approaching 1 mm. The results are discussed in relation to existing models of whisker reinforcement and published long-crack *T*-curve data. [Key words: bridging, composites, cracks, pullout, toughness.]

I. Introduction

THE incorporation of silicon carbide whiskers ($\approx 1 \mu\text{m}$ in diameter) into alumina can lead to considerable toughening.¹⁻⁸ A typical composite shows a monotonic toughness increase (toughness *T*-curve or crack-resistance *R*-curve) relative to $\approx 2.5 \text{ MPa} \cdot \text{m}^{1/2}$ for the base alumina, and maximum reported toughness values are 5 to 9 $\text{MPa} \cdot \text{m}^{1/2}$ (Refs. 8 to 11) depending on the properties and volume fraction of whiskers. It is generally accepted that the *T*-curve mechanisms involve some form of crack-interface bridging.⁸ However, the precise nature of these mechanisms remains an issue of much debate. Many argue, e.g., from near-tip observations using transmission electron microscopy,^{4,7} that the bridging primarily entails debonding and subsequent elastic deformation of the whiskers to abrupt rupture immediately (within 20 μm) behind the advancing crack tip. Those observations have been used as the basis for most micromechanics modeling.⁸ Few efforts have been made to reconcile such small-scale bridging zones with long-crack *T*-curve data (typical crack extension range $\approx 100 \mu\text{m}$ to 1 mm),⁹⁻¹¹ e.g., by invoking an artificially enhanced "tail" in the fiber-matrix constitutive stress-displacement function (associated with a distribution in whisker strengths) or secondary bridging from the alumina grains in a coarse-grained matrix.^{12,13}

In this communication we describe the results of some in situ experiments on crack growth in fine-grained alumina matrix materials reinforced with silicon carbide whiskers. The fine grain size minimizes potential bridging from the alumina grains themselves,^{12,13} in order that we may investi-

gate more clearly the micromechanisms of whisker toughening. Observations of whisker-bridging sites under load enable identification of these micromechanisms and, together with measurements of crack-opening displacements over the crack interface, indicate that the bridging which contributes to the toughness can indeed occur over substantial distances, i.e., up to 1 mm behind the crack tip. The results reveal the following features in the whisker-toughening process: (i) a considerably greater role of extended whisker pullout than hitherto proposed, (ii) identification of the *T*-curve baseline with the matrix (grain boundary) toughness, and (iii) enhancement of the bridge-formation processes from internal residual stresses.

I. Experimental Procedure

Two composites of silicon carbide whiskers[†] and alumina powder[‡] were hot-pressed as 50-mm-diameter disks at 1700°C for 1 h at a pressure of 42 MPa. Composite A was fabricated with 20 vol% whiskers that were 0.3 to 0.6 μm in diameter and 5 to 15 μm in length and composite B with 30 vol% whiskers that were 1.1 μm in diameter and 50 μm in length. The resultant composites achieved a density >99% with a random distribution of whiskers (except for slight alignment perpendicular to the hot-pressing direction) in matrices of grain size 1 to 2 μm .

The disks were surface ground to 1 mm in thickness and one surface of each was polished with diamond paste to 1- μm finish. Compact tension specimens with a notch of 7 mm in length and a tip radius of 150 μm were sawed from the disks.¹⁴ A tapered cut was made ahead of the notch from the back (unpolished) surface to produce a chevron guide ≈ 2 mm in length.¹⁴ This latter process was to provide extra stability in the ensuing crack extension. A Vickers indentation flaw (load 50 N) placed immediately ahead of the notch tip in the polished surface was then subjected to a preliminary load cycle to induce pop-in. The notch was finally resawed through the indentation, leaving a starter precrack $\approx 100 \mu\text{m}$ long.

The specimens were mounted into a fixture for in situ experiments in the scanning electron microscope (SEM)¹⁵ with the polished side facing the electron beam for direct observation of the crack trace. Loads applied externally to the specimen in the SEM enabled the crack to be stably propagated (if sometimes discontinuously) for distances up to ≈ 1 mm within the chevron. Individual bridging sites were monitored during the crack growth. Crack-opening displacements (COD) were measured behind the crack tip, to determine the bridged interface profiles.¹⁴

After running the crack through the chevron the specimens were withdrawn and resawed for repeat experiments.

K.T. Faber—contributing editor

Manuscript No. 196531. Received July 18, 1991; approved October 10, 1991.

Supported by the U.S. Air Force Office of Scientific Research and the U.S. Department of Energy.

*Member, American Ceramic Society.

†Guest scientist from the Department of Material Science and Engineering, Lehigh University, Bethlehem, PA. Now at the Technical University, Hamburg-Harburg, Hamburg, Germany.

‡TWS 100 (0.3 to 0.6 μm in diameter and 5 to 15 μm in length) and TWS 400 (1.1 μm in diameter, 50 μm in length), Tokai Carbon, Ltd., Tokyo, Japan.

§High-purity Reynolds alumina grade RC-HP DBM alumina powder with 0.05% MgO, mean particle size 0.5 μm and surface area 7.6 m²/g, Reynolds Metals Co., Richmond, VA.

III. Results

(1) Crack Propagation and Whisker Bridge Evolution

Specific examples of whisker bridging sites monitored in the SEM are shown in Figs. 1 and 2. Generally, the fracture followed an intergranular path in the alumina matrix with markedly abrupt deflections along or around the whiskers, although not always exactly along the whisker-matrix interfaces. These abrupt deflections appeared to be a most effective precursor to bridge formation. A majority of the whisker bridges ruptured at a distance $< 100 \mu\text{m}$ behind the crack tip, but some remained active over much greater distances. No detached microcracking at whisker-matrix interfaces more than a few grain diameters from the primary crack plane was observed.

Immediately behind the crack tip the walls begin to separate, but the whiskers remain mechanically connected across the interface. Figure 1(a) shows one such whisker $\approx 10 \mu\text{m}$ behind the tip, i.e., in the range ordinarily considered appropriate for "elastic" bridges.^{4,7} Many of the whiskers observed in our materials disengaged from the matrix within this range with little indication of pullout. However, the particular whisker in Fig. 1(a) remained intact prior to abrupt rupture until the tip had progressed $\approx 120 \mu\text{m}$ beyond the site, corresponding to a COD of $\approx 300 \text{ nm}$. Other bridges showed even longer range effects. Figure 1(b) shows one such site where the debonding and stress buildup was sufficient to cause secondary, off-plane matrix fragmentation around the embedded whisker $\approx 350 \mu\text{m}$ behind the crack tip. This implies a long tail to the bridging stress-separation function.

An even more striking example of a whisker with long-range interaction across the interface is shown in the sequence of Fig. 2. In this case the whisker is located only $\approx 70 \mu\text{m}$ from the mouth of the extending crack (i.e., from the notch tip). The whisker ruptures well away from the crack plane and pulls out (in apparently sustained frictional contact with the matrix over this distance) during monotonic loading, as shown in Figs. 2(a) to (c). The whisker is slightly inclined to the separation plane and, therefore, is subjected to increasing bending stresses during its pullout. As shown in Fig. 2(d), disengagement is $\approx 830 \mu\text{m}$ behind the crack tip, corresponding to a COD $\approx 1 \mu\text{m}$. The now unconstrained whisker rotates at its free end, so that, on unloading (Figs. 2(e) and (f)) the whisker does not re-enter its "socket" without some misfit, leaving the "closed" crack interface in a residual state of internal wedge loading.

(2) Crack-Opening Displacement (COD)

The COD measurements at the loaded crack interfaces allow us to construct the K -field plots in Fig. 3. We start with the Irwin relation¹⁴ for COD in terms of the stress-intensity factor K and coordinate x behind the crack tip:

$$u(x) = (8x/\pi)^{1/2} (1 - \nu^2) K/E \quad (1)$$

with Young's modulus $E \approx 400 \text{ GPa}$ and Poisson's ratio $\nu \approx 0.25$. This relation may reasonably be expected to hold in the region $x \leq \Delta c \ll c_0$ (recall crack extension $\Delta c \approx 1 \text{ mm}$ and notch length $c_0 \approx 7 \text{ mm}$ in our experiments) if the crack walls are stress free (i.e., zero bridging). In reality, the bridging K -field acts to restrain the crack walls from opening as wide as Eq. (1) predicts.

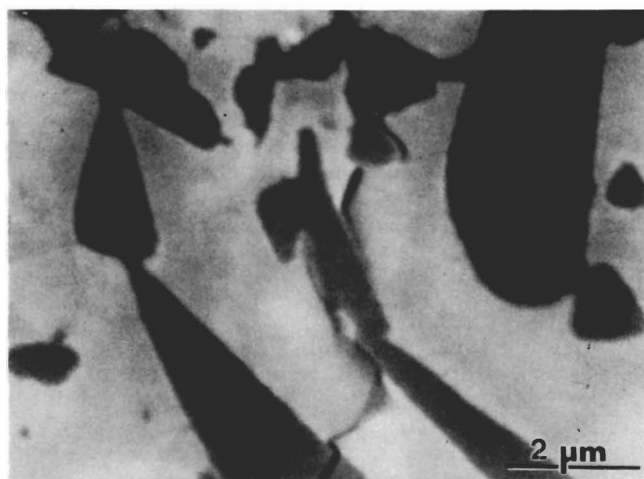
The $K[u(x)]$ data points shown in Fig. 3 are accordingly obtained by inversion of Eq. (1). The data in this figure indicate the K -field an "Irwinian" observer would measure on traversing the crack plane from crack tip ($x = 0$) to mouth ($x = \Delta c$). At $x = \Delta c$, $K = 5.1 \text{ MPa} \cdot \text{m}^{1/2}$ is an approximate (under)estimate of the unshielded, applied stress-intensity factor, corresponding to the limiting toughness at the long-crack plateau of the T -curve. At the extrapolated limit $x \rightarrow 0$, $K = 2.5 \text{ MPa} \cdot \text{m}^{1/2}$ represents the shielded, crack-tip stress-intensity factor and is close to the intrinsic grain-boundary toughness of the matrix alumina. This extrapolated value lies well below the minimum ($\approx 5 \text{ MPa} \cdot \text{m}^{1/2}$) measured by more conventional T -curve methods.⁸⁻¹¹ We note that the K -field is slightly greater for material B, i.e., the material with the higher density of coarser fibers. We also note that the K -field increases up to $x \approx 500 \mu\text{m}$, indicating a broad bridging zone and a corresponding long-range T -curve.^{14,8}

IV. Discussion

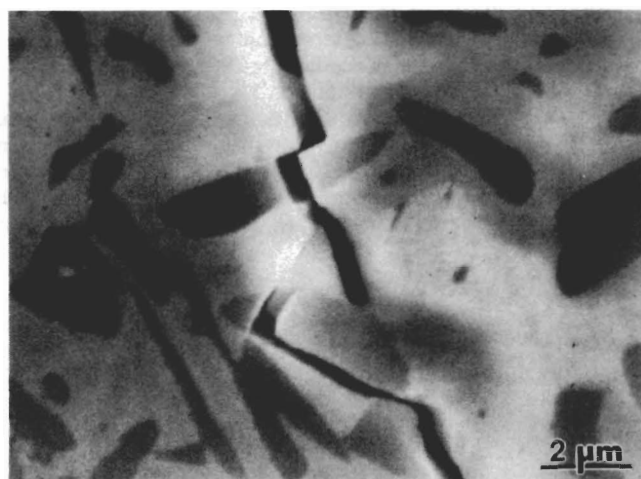
The present in situ observations enable us to identify more closely the bridging micromechanics of silicon carbide-whisker reinforcement in an alumina matrix, and to ascertain the range of the bridging zone.

For the bridging micromechanics, we see evidence for the short-range elastic component proposed in most analytical models.⁸ Local matrix stress is transferred to the progres-

⁸A complete, self-consistent analysis of the profile over the bridging zone is a complex numerical procedure,¹⁶ requiring (among other things) knowledge of the complete bridging-stress-separation function.



(a)



(b)

Fig. 1. In situ SEM micrographs of bridging silicon carbide whiskers in alumina for material B (crack direction downward). (a) Elastic bridge (central whisker) $10 \mu\text{m}$ behind crack tip. Note strong deflections at this bridge, not exactly along the whisker-matrix interface. (b) Mechanically interlocked whisker $350 \mu\text{m}$ behind the crack tip. Note adjoining microfracture in surrounding matrix at bridge site.

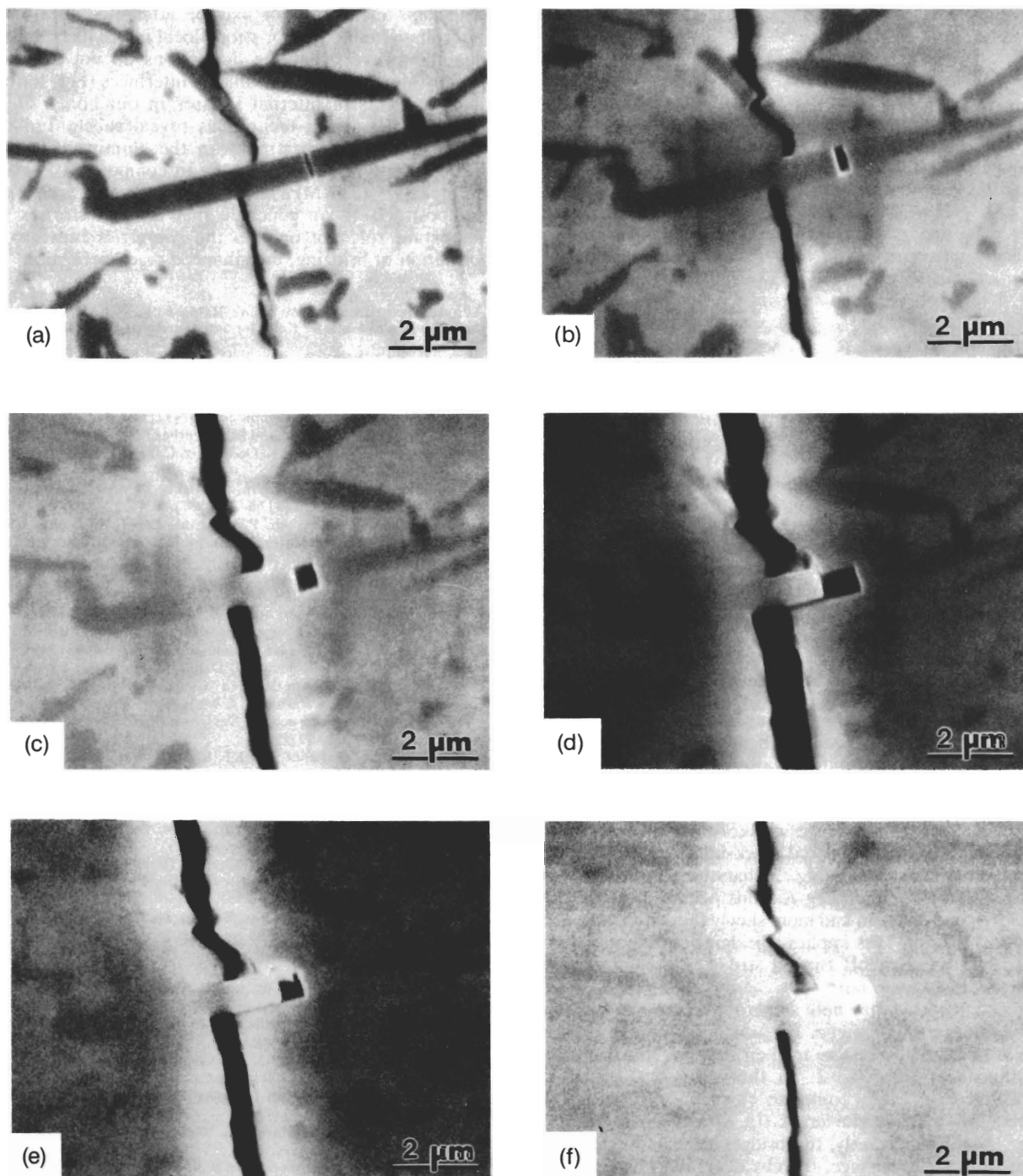


Fig. 2. In situ SEM sequence showing evolution of bridge whisker pullout for material A (crack direction downward). Distance x behind crack tip and force P on compact-tension load points: (a) $x = 100 \mu\text{m}$, $P = 167 \text{ N}$; (b) $x = 110 \mu\text{m}$, $P = 209 \text{ N}$; (c) $x = 330 \mu\text{m}$, $P = 213 \text{ N}$; (d) $x = 830 \mu\text{m}$, $P = 233 \text{ N}$; (e) $x = 830 \mu\text{m}$, $P = 101 \text{ N}$; and (f) $x = 830 \mu\text{m}$, $P = 0 \text{ N}$.

sively debonding whisker, until abrupt rupture occurs (whisker or matrix or both) in the near-crack plane. This rupture occurs most frequently at distances $x < 100 \mu\text{m}$ from the crack tip in our materials, with attendant energy dissipation by acoustic waves. However, in many instances, such as in Fig. 1, the rupture point is located much farther behind the crack tip than previously supposed.

However, even these unusually strong elastic bridges cannot account for the crack extension range of 1 mm or so that are apparent in the reported T -curve measurements.⁸⁻¹¹ Additionally, as may be deduced from indentation-flaw studies,¹⁷ the alumina grain size ($\approx 2 \mu\text{m}$) is far too small for a significant contribution from *matrix* grain-grain interlocking. Any explanation would require the extended cracks in our experi-

ments to be bridged over their entire lengths. Figure 2(c), where the bridge site remains active some $330 \mu\text{m}$ behind the crack tip, demonstrates the viability of such an extensive zone. An essential ingredient of persistent bridge activity is the substantial pullout that can occur well after whisker rupture. Although such pullout bridges constitute only a small fraction (perhaps 1 in 20) of observed sites in our observations, and the ensuing frictional tractions are unlikely to be as intense as those that build up at the rupture point, the toughness may be considerably enhanced by the relatively large crack-wall separation over which energy can be dissipated (corresponding to a large area under the stress-separation function). This frictional component of the work expenditure may be further augmented by enhanced wall-contact

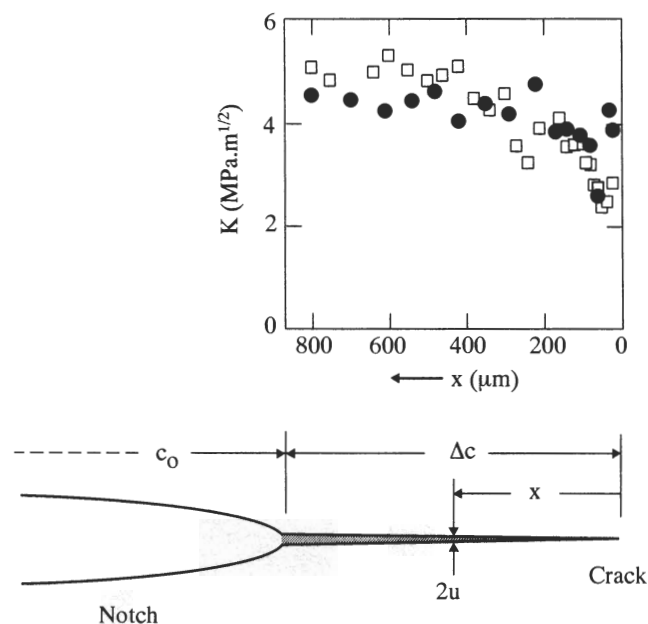


Fig. 3. K -field evaluated from crack-opening displacements along crack interface in silicon carbide-whisker-reinforced alumina for materials A (closed symbols) and B (open symbols). Cracks remain bridged (hatched region in schematic) in propagation through $\Delta c \approx 1000 \mu\text{m}$ (notch length $c_0 = 7 \text{ mm}$). Data points are K -field evaluations from inverted form of Irwin relation (Eq. (1)).

stresses associated with the oblique pullout in Fig. 2.^{18,19} On the other hand, the resulting bending moments on the bridges could cause premature failure of the whisker or matrix, e.g., Figs. 1(b) and 2(d), in part negating some of the potential benefits.

The importance of long-range whisker pullout interactions is also reflected in the measured crack-interface profile. We see from the COD data in Fig. 3 that the transition from crack tip to far-field bounding K -fields occurs most rapidly between $x = 0$ to $300 \mu\text{m}$, and more slowly thereafter between $x \approx 300$ to $1000 \mu\text{m}$. This implies a bridging stress-separation function with rapid falloff from a strong, short-range peak into a weak, long-range tail.

In this context, we may note some implications in our observations concerning fatigue. On unloading the crack the bridges are unlikely to restore to their original configuration at the interface, e.g., Fig. 2. At the very least, this may be expected to prevent complete closure, with resultant enhancement of the mean crack-tip K -field during cyclic loading.²⁰ More importantly, the bridges may suffer progressive and irreparable damage, thereby degrading the intrinsic toughening processes and reducing the lifetime.²¹

We reemphasize that the COD measurements provide a more accurate measure of the lower limit of the T -curve than do conventional fracture mechanics techniques. These latter techniques are restricted by the scale of the pop-in starter cracks (typically $100 \mu\text{m}$) used in the crack extension measurements. Here, extrapolation of our data to the crack tip ($x = 0$) in Fig. 3 yields $K \approx 2.5 \text{ MPa} \cdot \text{m}^{1/2}$, corresponding to the grain-boundary toughness, whereas the more conventional fracture mechanics methods are generally unable to obtain data below $K \approx 5 \text{ MPa} \cdot \text{m}^{1/2}$.⁸⁻¹¹

Finally, we may recall our observations in Section I(1) of markedly abrupt crack deflections in the proximity of

whiskers. Such behavior may be attributed to either weak interphase boundaries or strong local internal stresses. Recall again, however, that the deflections do not always occur exactly along the whisker-matrix interfaces (Fig. 1(a)). Direct measurements of internal stresses in our composites using neutron diffraction techniques reveal substantial thermal expansion mismatch stresses in the alumina ($\approx +200 \text{ MPa}$ in composite A and $+430 \text{ MPa}$ in composite B) and silicon carbide ($\approx -1330 \text{ MPa}$ in composite A and -1050 MPa in composite B).²² We conclude that residual stresses play an important role not only in the energetics but also in the formation of bridging, by enhanced crack deflection.

Acknowledgments: We thank Ralph F. Krause, Jr., for hot-pressing the samples and James F. Kelly for assistance with the SEM imaging.

References

1. P. F. Becher and G. C. Wei, "Toughening Behavior in SiC-Whisker Reinforced Alumina," *J. Am. Ceram. Soc.*, **67** [12] C-267-C-269 (1984).
2. J. Homeny, W. L. Vaughn, and M. K. Ferber, "Processing and Mechanical Properties of SiC-Whisker- Al_2O_3 -Matrix Composites," *Am. Ceram. Soc. Bull.*, **66** [2] 333-38 (1987).
3. J. Homeny and W. L. Vaughn, "Whisker-Reinforced Ceramic Matrix Composites," *MRS Bull.*, **7** [7] 66-71 (1987).
4. P. F. Becher, C.-H. Hsueh, P. Angelini, and T. N. Tieg, "Toughening Behavior in Whisker-Reinforced Ceramic Matrix Composites," *J. Am. Ceram. Soc.*, **71** [12] 1050-61 (1988).
5. P. F. Becher, "Recent Advances in Whisker-Reinforced Ceramics," *Annu. Rev. Mater. Sci.*, **20**, 179-95 (1990).
6. J. Homeny, W. L. Vaughn, and M. K. Ferber, "Silicon Carbide Whisker/Alumina Matrix Composites: Effect of Whisker Surface Treatment on Fracture Toughness," *J. Am. Ceram. Soc.*, **73** [2] 394-402 (1990).
7. G. H. Campbell, M. Rühle, B. J. Dalgleish, and A. G. Evans, "Whisker Toughening: A Comparison Between Aluminum Oxide and Silicon Nitride Toughened with Silicon Carbide," *J. Am. Ceram. Soc.*, **73** [3] 521-30 (1990).
8. P. F. Becher, "Microstructural Design of Toughened Ceramics," *J. Am. Ceram. Soc.*, **74** [2] 255-69 (1991).
9. R. F. Krause, E. R. Fuller, and J. F. Rhodes, "Fracture Resistance Behavior of Silicon Carbide Whisker-Reinforced Alumina Composites with Different Porosities," *J. Am. Ceram. Soc.*, **73** [3] 559-66 (1990).
10. J. Homeny and W. L. Vaughn, "R-Curve Behavior in a Silicon Carbide Whisker/Alumina Matrix Composite," *J. Am. Ceram. Soc.*, **73** [7] 2060-62 (1990).
11. S. V. Nair, "Crack-Wake Debonding and Toughness in Fiber- or Whisker-Reinforced Brittle-Matrix Composites," *J. Am. Ceram. Soc.*, **73** [10] 2839-47 (1990).
12. P. L. Swanson, C. J. Fairbanks, B. R. Lawn, Y-W Mai, and B. J. Hockey, "Crack-Interface Grain Bridging as a Fracture Resistance Mechanism in Ceramics: I. Experimental Study on Alumina," *J. Am. Ceram. Soc.*, **70** [4] 279-89 (1987).
13. P. F. Becher, E. R. Fuller, Jr., and P. Angelini, "Matrix-Grain-Bridging Contributions to the Toughness of Whisker-Reinforced Ceramics," *J. Am. Ceram. Soc.*, **74** [9] 2131-35 (1991).
14. J. Rödel, J. F. Kelly, and B. R. Lawn, "In Situ Measurements of Bridged Crack Interfaces in the SEM," *J. Am. Ceram. Soc.*, **73** [11] 3313-18 (1990).
15. J. Rödel, J. F. Kelly, M. R. Stoudt, and S. J. Bennison, "A Loading Device for Fracture Testing of Compact Tension Specimens in the SEM," *Scanning Microsc.*, **5** [1] 29-35 (1991).
16. B. N. Cox and D. B. Marshall, "Determination of Crack Bridging Forces," *Int. J. Fract.*, in press.
17. P. Chantikul, S. J. Bennison, and B. R. Lawn, "Role of Grain Size in the Strength and R-Curve Properties of Alumina," *J. Am. Ceram. Soc.*, **73** [8] 2419-27 (1990).
18. J. Bowling and G. W. Groves, "The Debonding and Pullout of Ductile Wires from a Brittle Matrix," *J. Mater. Sci.*, **14** [2] 431-42 (1979).
19. V. C. Li, Y. Wang, and S. Backer, "Effect of Inclining Angle, Bundling and Surface Treatment on Synthetic Fibre Pull-Out From a Cement Matrix," *Composites (Guildford U.K.)*, **21** [2] 132-40 (1990).
20. R. O. Ritchie, "Mechanisms of Fatigue Crack Propagation in Metals, Ceramics and Composites: Role of Crack Tip Shielding," *Mater. Sci. Eng.*, **A103** [2] 15-28 (1988).
21. S. Lathabai, J. Rödel, and B. R. Lawn, "Cyclic Fatigue from Frictional Degradation at Bridging Grains in Alumina," *J. Am. Ceram. Soc.*, **74** [6] 1340-48 (1991).
22. H. Prask, C. Choi, E. R. Fuller, R. F. Krause, A. Krawitz, and J. Richardson, "Micro-Stresses in Ceramic Composites," Annual Report, NIST Reactor Radiation Division, 1990. □